Flatness-based control of open-channel flow in an irrigation canal using SCADA

T. Rabbani, S. Munier, D. Dorchies, P.O. Malaterre, Aurélie Bayen-Poisson, X. Litrico

Author-produced version of the article published in IEEE Control Systems Magazine, 2009, 29(5), 22-30.
The original publication is available at http://ieeexplore.ieee.org/
doi : 10.1109/MCS.2009.933524

Flatness-Based Control of Open-Channel Flow in an Irrigation Canal Using SCADA

Tarek Rabbani, Simon Munier, David Dorchies, Pierre-Olivier Malaterre,

Alexandre Bayen and Xavier Litrico — June 13, 2009

With a population of more than six billion people, food production from agriculture must be raised to meet increasing demand. While irrigated agriculture provides 40% of the total food production, it represents 80% of the freshwater consumption worldwide. In summer and drought conditions, efficient management of scarce water resources becomes crucial. The majority of irrigation canals are managed manually, however, with large water losses leading to low water efficiency. The present article focuses on the development of algorithms that could contribute to more efficient management of irrigation canals that convey water from a source, generally a dam or reservoir located upstream, to water users. We also describe the implementation of an algorithm for real-time irrigation operations using a *supervision, control, and data acquisition* (SCADA) system with automatic centralized controller.

Irrigation canals can be viewed and modeled as delay systems since it takes time for the water released at the upstream end to reach the user located downstream. We thus present an open-loop controller that can deliver water at a given location at a specified time. The development of this controller requires a method for inverting the equations that describe the dynamics of the canal in order to parameterize the controlled input as a function of the desired output. The

Author-produced version of the article published in IEEE Control Systems Magazine, 2009, 29(5), 22-30.
The original publication is available at http://ieeexplore.ieee.org/
doi : 10.1109/MCS.2009.933524

Saint-Venant equations [1] are widely used to describe water discharge in a canal. Since these equations are not easy to invert, we use a simplified model, called the Hayami model. We use differential flatness to invert the dynamics of the system and to design an open-loop controller.

Modeling Open Channel Flow

Saint-Venant Equations

The Saint-Venant equations for water discharge in a canal are named after Adhémar Jean-Claude Barré de Saint-Venant, who derived these equations in 1871 [1]. This model assumes one-dimensional flow, with uniform velocity over the cross section of the canal. The effect of boundary friction is accounted for through an empirical law such as the Manning-Strickler friction law [2]. The average canal bed slope is assumed to be small, and the pressure is assumed to be hydrostatic. Under these assumptions, the Saint-Venant equations are given by

$$\frac{\partial A}{\partial t} + \frac{\partial Q}{\partial x} = 0, \tag{1}$$

$$\frac{\partial Q}{\partial t} + \frac{\partial \left(Q^2/A\right)}{\partial x} + gA\frac{\partial H}{\partial x} = gA(S_b - S_f), \tag{2}$$

where $A(x,t)$ is the wetted cross-sectional area, $Q(x,t)$ is the water discharge $(\mathrm{m}^3/\mathrm{s})$ through the cross section $A(x,t)$, $H(x,t)$ is the water depth, $S_f(x,t) = \frac{Q^2 n^2}{A^2 R^{4/3}}$ is the dimensionless friction slope, $R(x,t) = \frac{A}{P}$ is the hydraulic radius (m), $P(x,t)$ is the wetted perimeter (m), n is the Manning coefficient $(\mathrm{s\text{-}m}^{-1/3})$, S_b is the bed slope $(\mathrm{m/m})$, and g is the gravitational acceleration $(\mathrm{m/s}^2)$. Equation (1) expresses conservation of mass, while (2) expresses conservation of momentum.

Equations (1), (2) are completed by boundary conditions at cross structures, such as

Author-produced version of the article published in IEEE Control Systems Magazine, 2009, 29(5), 22-30.
The original publication is available at http://ieeexplore.ieee.org/
doi : 10.1109/MCS.2009.933524

gates or weirs, where the Saint-Venant equations are not valid. Figure 1 illustrates some of the Saint-Venant equations parameters and shows a gate cross structure. The cross structure at the downstream end of the canal can be modeled by a static relation between the water discharge $Q(L,t)$ and the water depth $H(L,t)$ at $x = L$ given by

$$Q(L,t) = W(H(L,t)), \tag{3}$$

where $W(\cdot)$ is derived from hydrostatic laws. For a weir overflow structure, this relation is given by

$$Q(L,t) = C_w\sqrt{2g}L_w\left(H(L,t) - H_w\right)^{3/2},$$

where g is the gravitational acceleration, L_w is the weir length, H_w is the weir elevation, and C_w is the weir discharge coefficient.

A Simplified Linear Model

A simplified version of the Saint-Venant equations is obtained by neglecting the inertia terms $\frac{\partial Q}{\partial t} + \frac{\partial\left(Q^2/A\right)}{\partial x}$ in the momentum equation (2), which leads to the diffusive wave equation [3]. Linearizing the Saint-Venant equations about a nominal water discharge Q_0 and water depth H_0 yields the Hayami equations

$$D_0\tfrac{\partial^2 q}{\partial x^2} - C_0\tfrac{\partial q}{\partial x} = \frac{\partial q}{\partial t}, \tag{4}$$

$$B_0\tfrac{\partial h}{\partial t} + \tfrac{\partial q}{\partial x} = 0, \tag{5}$$

where $C_0 = C_0(Q_0)$ and $D_0 = D_0(Q_0)$ are, respectively, the nominal wave celerity and diffusivity, which depend on Q_0, and B_0 is the average bed width. The quantities $q(x,t)$ and $h(x,t)$ are the deviations from the nominal water discharge and water depth, respectively. Figure 2 illustrates the relevant notation.

Author-produced version of the article published in IEEE Control Systems Magazine, 2009, 29(5), 22-30.
The original publication is available at http://ieeexplore.ieee.org/
doi : 10.1109/MCS.2009.933524

The linearized boundary condition at the downstream end $x = L$ is given by

$$q(L,t) = bh(L,t), \tag{6}$$

where $b = \frac{\partial W}{\partial H}(H_0)$ is the linearization constant. The value of b depends on the hydraulic structure geometry, including its length, height, and discharge coefficient of the weir. The initial conditions are defined by the deviations from their nominal values, which are assumed to be zero initially, that is,

$$q(x,0) \quad = 0, \tag{7}$$

$$h(x,0) \quad = 0. \tag{8}$$

Flatness-based Open-loop Control

Open-loop Control of a Canal Pool

We develop a feedforward controller for water discharge in an open-channel hydraulic system. The system of interest is a hydraulic canal with a cross structure at the downstream end as shown in Figure 2. We assume that the desired downstream downstream water discharge $q_{\mathrm{d}}(t)$ is specified in advance based on scheduled user demands. The control problem consists of determining the upstream water discharge $q(0,t)$ that has to be delivered in order to meet the desired downstream water discharge $q_{\mathrm{d}}(t)$. This inverse problem is an open-loop control problem. Note that, by linearization, computing $q(0,t)$ as a function of $q_d(t)$ is equivalent to determining $Q(0,t)$ as a function of $Q_{\mathrm{d}}(t) = Q_0 + q_{\mathrm{d}}(t)$.

The upstream water discharge $q(0,t)$ is the solution of the open-loop control problem

Author-produced version of the article published in IEEE Control Systems Magazine, 2009, 29(5), 22-30.
The original publication is available at http://ieeexplore.ieee.org/
doi : 10.1109/MCS.2009.933524

defined by the Hayami model equations (4), (5), initial conditions (7), (8), and boundary condition (6). Differential flatness, as described in "What is Differential Flatness?", provides a way to solve this open-loop control problem [3], [4] in the form of a parameterization of the input $u(t) = q(0,t)$ as a function of the desired output $y(t) = q_{\mathrm{d}}(t)$. Specifically it is proved in [3], [4], that the controller can be expressed in closed form as

$$u(t) = e^{\left(-\frac{\alpha^2}{\beta^2}t - \alpha L\right)} \left(T_1(t) - \kappa T_2(t) + \frac{B_0}{b} T_3(t) \right), \tag{9}$$

where the T_1, T_2, and T_3 are given by

$$T_1(t) \triangleq \sum_{i=0}^{\infty} \frac{d^i(e^{\frac{\alpha^2}{\beta^2}t} y(t))}{dt^i} \frac{\beta^{2i} L^{2i}}{(2i)!}, \tag{10}$$

$$T_2(t) \triangleq \sum_{i=0}^{\infty} \frac{d^i(e^{\frac{\alpha^2}{\beta^2}t} y(t))}{dt^i} \frac{\beta^{2i} L^{2i+1}}{(2i+1)!}, \tag{11}$$

$$T_3(t) \triangleq \sum_{i=0}^{\infty} \frac{d^{i+1}(e^{\frac{\alpha^2}{\beta^2}t} y(t))}{dt^{i+1}} \frac{\beta^{2i} L^{2i+1}}{(2i+1)!}, \tag{12}$$

$\alpha \triangleq \frac{C_0}{2D_0}$, $\beta \triangleq \frac{1}{\sqrt{D_0}}$, and $\kappa \triangleq \frac{B_0}{b}\frac{\alpha^2}{\beta^2} - \alpha$. We call (9) the Hayami controller.

The convergence of the infinite series (10)-(12) can be guaranteed when the desired output function $y(t)$ and its derivatives are bounded in a specific sense. More specifically, the infinite series (9) converges when the desired output $y(t) = q_{\mathrm{d}}(t)$ is a Gevrey function of order r lower than 2 [3], [4]. A Gevrey function $y(t)$ is defined by the following property. For all nonnegative n, the n^{th} derivative $y^{(n)}(t)$ of a Gevrey function $y(t)$ of order r has bounded derivatives that satisfy

$$\sup_{t \in [0,T]} \left| y^{(n)}(t) \right| < m \frac{(n!)^r}{l^n},$$

where m and l are constant positive scalars independent of n.

Author-produced version of the article published in IEEE Control Systems Magazine, 2009, 29(5), 22-30.
The original publication is available at http://ieeexplore.ieee.org/
doi : 10.1109/MCS.2009.933524

Assessment of the Performance of the Method in Simulation

Before field implementation, it is necessary to test the method in simulation. We simulate the Hayami controller (9), on the nonlinear Saint-Venant model.

Simulation of Irrigation Canals

The simulations are carried out using the software package Simulation of Irrigation Canals (SIC) [5], which implements a semi-implicit Preissmann scheme to solve the nonlinear Saint-Venant equations (1), (2) for open-channel one-dimensional flow [5], [6]. Instead of defining a fictitious canal, we use a realistic geometry corresponding to a stretch of the Gignac canal (see description below) to evaluate the open-loop control in simulation. The considered stretch is 4940 m long, with an average bed slope $S_b = 3.8 \times 10^{-4}$ m/m, an average bed width $B_0 = 2$ m, and Manning coefficient $n = 0.024$ s-m$^{-1/3}$.

Parameter Identification

The simulations are performed on a realistic canal geometry, which is neither prismatic nor uniform. Consequently, it is not possible to express C_0, D_0, and b analytically in terms of the physical parameters such as the canal geometry and water discharge. For this reason, it is necessary to empirically estimate the parameters C_0, D_0, and b of the Hayami model that would best approximate the water discharge governed by the Saint-Venant equations (1), (2). The identification is done with an upstream water discharge in the form of a step input. The water discharges are monitored at the upstream and downstream positions. The identification

Author-produced version of the article published in IEEE Control Systems Magazine, 2009, 29(5), 22-30.
The original publication is available at http://ieeexplore.ieee.org/
doi : 10.1109/MCS.2009.933524

is performed by finding the parameter values that minimize the least-squares error between the downstream water discharge computed by the Hayami model and the downstream water discharge simulated by SIC. The identification is performed using data generated by simulating the Saint-Venant equations around a nominal water discharge $Q_0 = 0.400$ m^3/s. The identification leads to the parameters $C_0 = 0.84$ m/s, $D_0 = 634$ m^2/s, and $b = 0.61$ m^2/s.

Desired Water Demand

The water demand curve is approximated from predicted consumption or by information from farmers about their consumption intentions. User consumption requirements at offtakes are usually modeled by a demand curve in the form of a step function. However, depending on the canal model used, this demand may require high values of upstream water discharge. We define the demand curve to be a linear transformation of a Gevrey function of the form $y(t) = q_1\phi_\sigma(t/T)$, where q_1 and T are constants, and $\phi_\sigma(t)$ is a Gevrey function of order $1+1/\sigma$ called the dimensionless bump function. The chosen Gevrey function allows a transition from zero water discharge for $t \leq 0$ to a water discharge equal to q_1 for $t \geq T$. The function $\phi_\sigma(t)$ is illustrated in Figure 3 for various values of σ.

Simulation Results

The Hayami control (9) is computed using the estimated parameters C_0, D_0, and b. The downstream water discharge is defined by $y(t) = q_1\phi_\sigma(t/T)$, where $q_1 = 0.1$ m^3/s, $\sigma = 1.4$, and $T = 3$ h. Figure 4 shows the control $u(t)$ and the desired output $y(t)$.

The upstream water discharge (9) is simulated with SIC to compute the corresponding

Author-produced version of the article published in IEEE Control Systems Magazine, 2009, 29(5), 22-30.
The original publication is available at http://ieeexplore.ieee.org/
doi : 10.1109/MCS.2009.933524

downstream water discharge. Figure 5 shows the downstream water discharge and the desired downstream water discharge.

Although the open-loop control is based on the linear Hayami model, the relative error between the downstream water discharge and the desired downstream water discharge, defined by $e_{\text{rel}}(t) = \left|\frac{q(L,t)-y(t)}{Q_0}\right|$, is less than 0.3%.

Implementation on the Gignac Canal in Southern France

Experiments are performed on the Gignac Canal, located northwest of Montpellier, in southern France. The main canal is 50 km long, with a feeder canal, 8 km long, and two branches on the left and right banks of Hérault river, 27 km and 15 km long, respectively. Figure 6 shows a map of the feeder canal with its left and right branches.

As shown in Figure 7a, the canal separates at Partiteur station into two branches, namely, the right branch and the left branch. The canal is equipped at each branch with an automatic regulation gate with position sensors as shown in Figure 7b. Piezoresistive sensors are used to measure the water level by measuring the resistance in the sensor wires. An ultrasonic velocity sensor measures the average water velocity, see Figure 7c. The velocity measurement, water-level measurement, and the geometric properties of the canal at the gate determine the water discharge.

We are interested in controlling the water discharge into the right branch of the canal. The cross section of the right branch is trapezoidal with average bed slope $S_b = 0.00035$ m/m. The Gignac canal is equipped with a SCADA system, which enables the implementation of

Author-produced version of the article published in IEEE Control Systems Magazine, 2009, 29(5), 22-30.
The original publication is available at http://ieeexplore.ieee.org/
doi : 10.1109/MCS.2009.933524

controllers. Data from sensors and actuators of the four gates at Partiteur are collected by a control station at the left branch as shown in Figure 8. The information is communicated by radio frequency signals every five minutes to a receiving antenna, located in the main control center, a few kilometers away. The data are displayed and saved in a database, while commands to the actuators are sent back to the local controllers at the gates. We use the SCADA system to perform open-loop control in real time. In this experiment, we are interested in controlling the gate at the right branch of the Partiteur station to achieve a desired water discharge five kilometers downstream at Avencq station. The gate opening at Partiteur is computed to deliver the upstream water discharge; for details, see "How to Impose a Discharge at a Gate?".

Results Obtained Assuming Constant Lateral Withdrawals

We now estimate the canal parameters for the canal between Partiteur and Avencq. The nominal water discharge is $Q_0 = 0.640$ m^3/s. The identification is done using real sensor data, and leads to the estimates $C_0 = 1.35$ m/s, $D_0 = 893$ m^2/s, and $b = 0.17$ m^2/s. We define a downstream water discharge by $y(t) = q_1\phi_\sigma(t/T)$, where $q_1 = -0.1$ m^3/s, $\sigma = 1.4$, and $T = 3.2$ h. The upstream water discharge is computed using (9). Figure 9 shows the desired downstream water discharge and the upstream water discharge, to be applied at the upstream with the measured discharges at each location, respectively.

The actuator limitations include a deadband in the gate opening of 2.5 cm and unmodeled disturbances such as friction in the gate-opening mechanism. Although the downstream water discharge is tracked well until $t \approx 3.4$ h, a steady-state error of 0.03 m^3/s is evident. This error does not seem to be due to the actuator limitations, but rather to simplifications in the

Author-produced version of the article published in IEEE Control Systems Magazine, 2009, 29(5), 22-30.
The original publication is available at http://ieeexplore.ieee.org/
doi : 10.1109/MCS.2009.933524

model assumptions, not necessarily satisfied in practice. In particular, we assume constant lateral withdrawals, whereas in reality the lateral withdrawals are driven by gravity. Such gravitational lateral withdrawals vary with the water level, as opposed to lateral withdrawals by pumps, which can be assumed constant.

Modeling the Effects of Gravitational Lateral Withdrawals

The gravitational lateral withdrawals in an offtake are a function of the water level in the canal just upstream of the offtake. Typically, the flow through an underflow offtake is proportional to the square root of the upstream water level. As a first approximation, we linearize this relation, and assume that the offtakes are located at the downstream end of the canal. Then, instead of being constant, the lateral flow is proportional to the downstream water level. The downstream gravitational lateral withdrawals can be seen as a local feedback between the level and the water discharge. The dynamical model of the canal is then modified as

$$q_{\text{lateral}}(t) = b_1 h(L,t), \tag{13}$$

where b_1 is the linearization constant of gravitational lateral withdrawals. We combine the output equation $y(t) = q_{\text{d}}(t) = bh(L,t)$ with the conservation of water discharge at $x = L$, given by $q(L,T) = q_{\text{lateral}}(t) + q_{\text{d}}(t) = (b + b_1)h(L,t)$, to obtain

$$y(t) = Gq(L,t),$$

where $G = \frac{b}{b+b_1}$. The effect of gravitational lateral withdrawals is thus expressed by a gain factor G, which is less than 1. This gain factor G explains why the released upstream water discharge must be larger than the desired downstream water discharge to account for the gravitational lateral withdrawals. The control (9) does not account for the gain factor G, which leads to a

Author-produced version of the article published in IEEE Control Systems Magazine, 2009, 29(5), 22-30.
The original publication is available at http://ieeexplore.ieee.org/
doi : 10.1109/MCS.2009.933524

steady-state error in the downstream water discharge. Feedback control can provide a solution for this steady-state error by including an integral control component. However, since we are using open-loop control, we need to include the gain-factor effect in this controller to reduce the steady-state error.

The open-loop control is deduced by replacing b with $b_{\text{eq}} = b + b_1$ in both (9) and the expression for κ, and replacing $y(t)$ by $q(L,t) = G^{-1}y(t)$. The open-loop control for the gravitational lateral withdrawals case is

$$u_{\text{gravitational}}(t) = \frac{1}{G} e^{\left(-\frac{\alpha^2}{\beta^2}t - \alpha L\right)} \left(T_1(t) - \kappa T_2(t) + \frac{B_0}{b_{\text{eq}}} T_3(t) \right). \tag{14}$$

In the case of gravitational lateral withdrawals, the open-loop control depends on the parameters G, C_0, D_0, and b_{eq}. These parameters are estimated using the same method outlined for the constant lateral withdrawals.

Results Obtained Accounting for Gravitational Lateral Withdrawals

The Saint-Venant equations with the open-loop control input are simulated using SIC software, in order to evaluate the impact of gravitational lateral withdrawals on the output.

Simulation Results

The simulations are carried out on a test canal of length $L = 4940$ m, average bed slope $S_b = 3.8 \times 10^{-4}$, average bed width $B_0 = 2$ m, Manning coefficient $n = 0.024$ s-m$^{-1/3}$, and gravitational lateral withdrawals distributed along its length. Identification is performed about a nominal water discharge $Q_0 = 0.400$ m^3/s. The identification leads to the parameter estimates

Author-produced version of the article published in IEEE Control Systems Magazine, 2009, 29(5), 22-30.
The original publication is available at http://ieeexplore.ieee.org/
doi : 10.1109/MCS.2009.933524

$G = 0.90$, $C_0 = 0.87$ m/s, $D_0 = 692.34$ m^2/s, and $b_{\text{eq}} = 0.62$ m^2/s for the gravitational lateral withdrawals, and to $C_0 = 0.84$ m/s, $D_0 = 1100.72$ m^2/s, and $b = 0.75$ m^2/s for the constant lateral withdrawals. The downstream water discharge is defined by $y(t) = q_1\phi_\sigma(t/T)$, where $q_1 = 0.1$ m^3/s, $\sigma = 1.4$, and $T = 8$ h. Figure 10 shows the upstream water discharge $u(t)$ and $u_{\text{gravitational}}(t)$ for constant and gravitational lateral withdrawals, respectively.

We notice that the open-loop control that accounts for gravitational lateral withdrawals has a steady-state above the desired output to compensate for the variable withdrawal of water. The upstream water discharge $u(t)$ is simulated with SIC to compute the corresponding downstream water discharge. Figure 11 shows the SIC simulation results.

Experimental Results

Estimation of the canal parameters between Partiteur and Avencq is performed as described above for the Hayami model that accounts for gravitational lateral withdrawals. The nominal water discharge is $Q_0 = 0.480$ m^3/s. The identified parameters of the Hayami model are $G = 0.70$, $C_0 = 1.08$ m/s, $D_0 = 444$ m^2/s, and $b = 0.27$ m^2/s. The downstream water discharge is defined by $y(t) = q_1\phi(t/T)$, where $q_1 = 0.1$ m^3/s, $\sigma = 1.4$, and $T = 5$ h. The upstream water discharge $u_{\text{gravitational}}(t)$ is computed using (14). Figure 12 shows the desired downstream water discharge, the numerical control computed by (14), the experimental control achieved by the physical system, and the measured downstream water discharge. The relative error between the measured downstream water discharge and the desired downstream water discharge is less than 9%, despite the fact that the delivered upstream water discharge is perturbed due to actuator limitations.

Author-produced version of the article published in IEEE Control Systems Magazine, 2009, 29(5), 22-30.
The original publication is available at http://ieeexplore.ieee.org/
doi : 10.1109/MCS.2009.933524

Conclusion

This article applied a flatness-based controller for an open channel hydraulic canal. The controller was tested by computer simulation using Saint-Venant equations as well as by real experimentation on the Gignac canal in southern France. The initial model that assumes constant lateral withdrawals is improved to take into account gravitational lateral withdrawals, which vary with the water level. Accounting for gravitational lateral withdrawals decreased the steady-state error from 6.2% (constant lateral withdrawals assumption) to 1% (gravitational lateral withdrawals assumption). The flatness-based open-loop controller is thus able to compute the upstream water discharge corresponding to a desired downstream water discharge, taking into account the gravitational withdrawals along the canal reach.

Acknowledgments

Financial help of the France-Berkeley Fund is gratefully acknowledged. We thank Céline Hugodot, Director of the Canal de Gignac for her help concerning the experiments.

Author-produced version of the article published in IEEE Control Systems Magazine, 2009, 29(5), 22-30.
The original publication is available at http://ieeexplore.ieee.org/
doi : 10.1109/MCS.2009.933524

References

[1] A. J. C. Barré de Saint-Venant. Théorie du mouvement non-permanent des eaux avec application aux crues des rivières à l'introduction des marées dans leur lit. *Comptes rendus de l'Académie des Sciences*, 73:148–154, 237–240, 1871.

[2] T. Sturm. *Open channel hydraulics*. McGraw-Hill Science Engineering, New York, NY, 2001.

[3] T. Rabbani, F. Di Meglio, X. Litrico, and A. Bayen. Feed-forward control of open channel flow using differential flatness. *IEEE Transactions on Control Systems Technology*, to appear 2009.

[4] F. Di Meglio, T. Rabbani, X. Litrico, and A. Bayen. Feed-forward river flow control using differential flatness. *Proceedings of the 47th IEEE Conference on Decision and Control, Cancun, Mexico*, 1:3903–3910, December 2008.

[5] J.-P. Baume, P.-O. Malaterre, G. Belaud, and B. Le Guennec. SIC: a 1D hydrodynamic model for river and irrigation canal modeling and regulation. *Métodos Numéricos em Recursos Hidricos*, 7:1–81, 2005.

[6] P.-O. Malaterre. SIC 4.20, simulation of irrigation canals, 2006. http://www.canari.free.fr/sic/sicgb.htm.

Author-produced version of the article published in IEEE Control Systems Magazine, 2009, 29(5), 22-30.
The original publication is available at http://ieeexplore.ieee.org/
doi : 10.1109/MCS.2009.933524

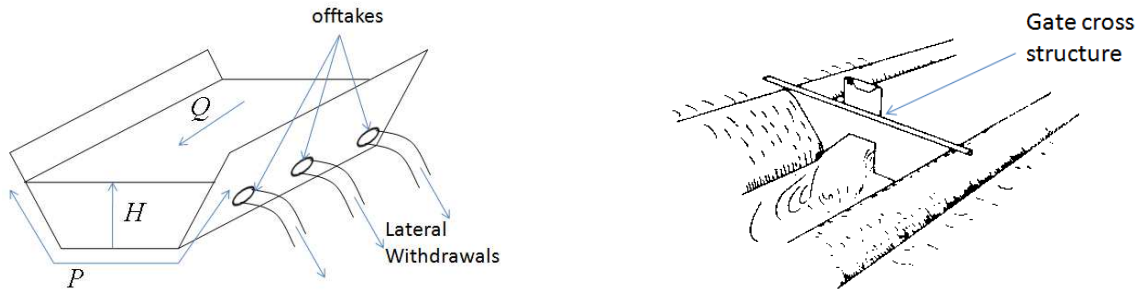

(a) (b)

Figure 1: Irrigation canal. (a) shows the flow Q, water depth H, and wetted perimeter P. Lateral withdrawals are taken from offtakes. (b) shows a gate cross structure, which can be used to control the water discharge in the canal.

Author-produced version of the article published in IEEE Control Systems Magazine, 2009, 29(5), 22-30.
The original publication is available at http://ieeexplore.ieee.org/
doi : 10.1109/MCS.2009.933524

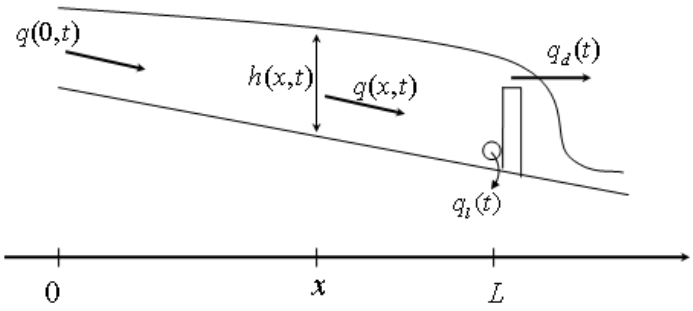

Figure 2: Longitudinal schematic profile of a hydraulic canal. A canal is a structure that directs water flow from an upstream location to a downstream location. Water offtakes are assumed to be located at the downstream of the canal. The variables $q(x,t)$, $h(x,t)$, $q_{\mathrm{d}}(t)$, and $q_{\mathrm{l}}(t)$ are the deviations from the nominal values of water discharge, water depth, desired downstream water discharge, and lateral withdrawal, respectively.

Author-produced version of the article published in IEEE Control Systems Magazine, 2009, 29(5), 22-30.
The original publication is available at http://ieeexplore.ieee.org/
doi : 10.1109/MCS.2009.933524

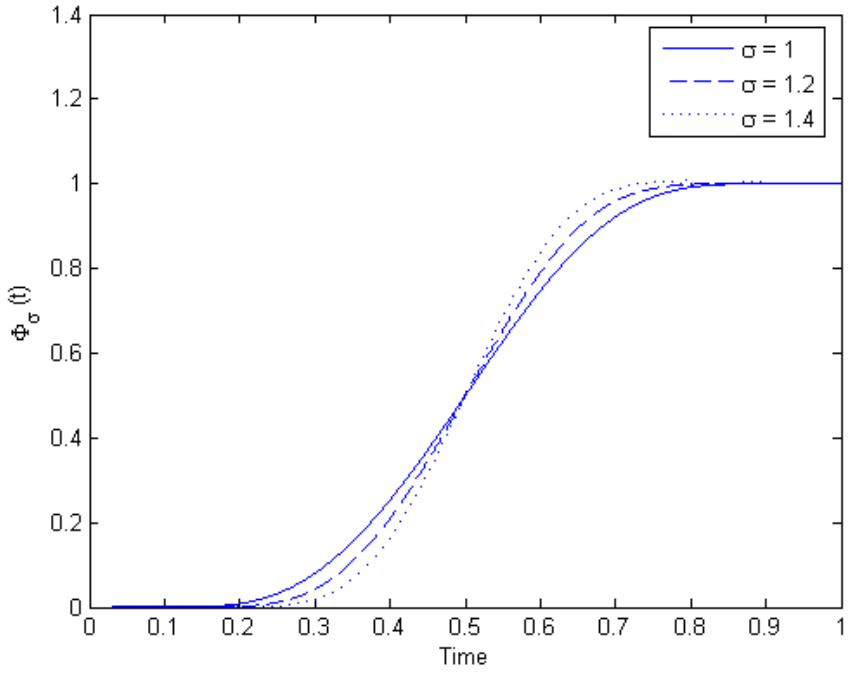

Figure 3: Dimensionless bump function. The bump function $\phi_\sigma(t)$ is a Gevrey function of order $1 + 1/\sigma$.

Author-produced version of the article published in IEEE Control Systems Magazine, 2009, 29(5), 22-30.
The original publication is available at http://ieeexplore.ieee.org/
doi : 10.1109/MCS.2009.933524

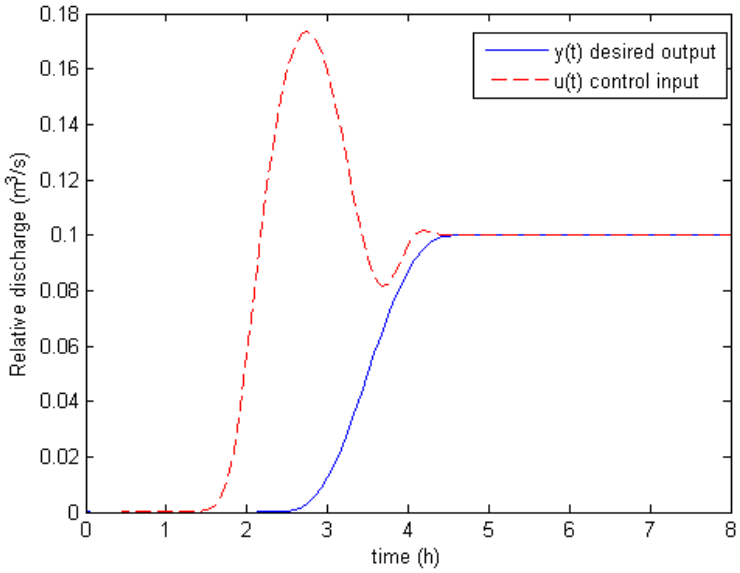

Figure 4: Hayami control input signal. The control input $u(t) = q(0,t)$ is computed using the differential flatness method applied to the Hayami model for the desired downstream water discharge $y(t)$.

Author-produced version of the article published in IEEE Control Systems Magazine, 2009, 29(5), 22-30.
The original publication is available at http://ieeexplore.ieee.org/
doi : 10.1109/MCS.2009.933524

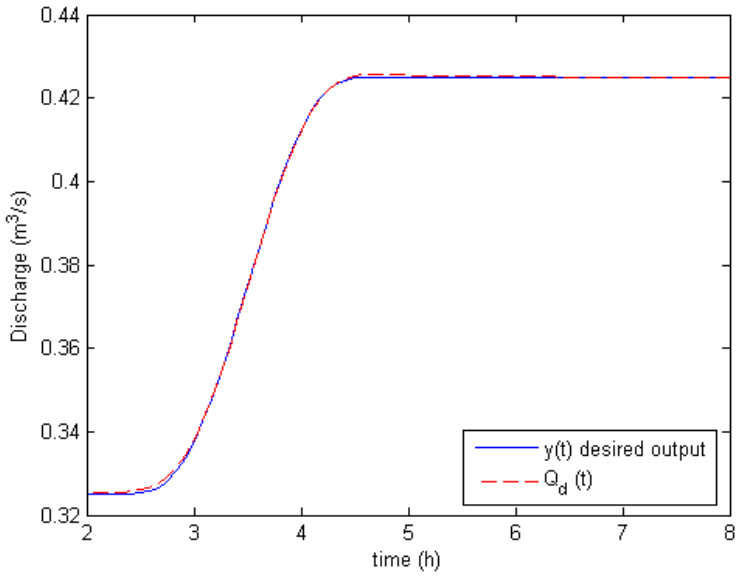

Figure 5: Hayami-model-based control applied to the Saint-Venant model. The downstream water discharge is computed using SIC software. The downstream water discharge $Q_{\mathrm{d}}(t)$ is the output obtained by applying the Hayami control on the full nonlinear model (Saint-Venant model). Although the open-loop control is based on the Hayami model, the relative error between the downstream water discharge and the desired downstream water discharge is less than 0.3%.

Author-produced version of the article published in IEEE Control Systems Magazine, 2009, 29(5), 22-30.
The original publication is available at http://ieeexplore.ieee.org/
doi : 10.1109/MCS.2009.933524

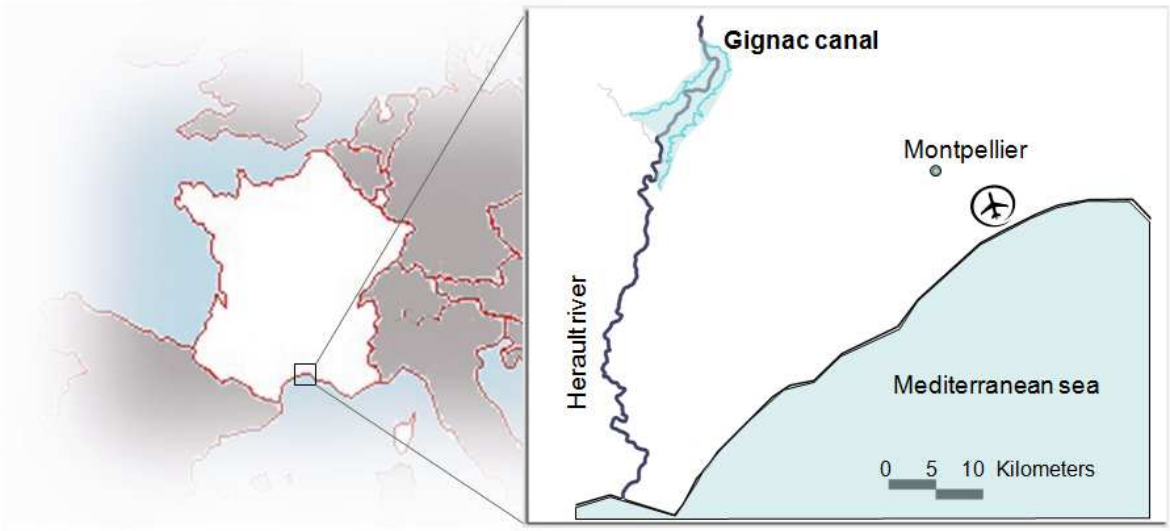

Figure 6: Location of the Gignac canal in southern France. The canal takes water from the Hérault river to feed two branches that irrigate a total area of 3000 hectare, where vineyards are located.

Author-produced version of the article published in IEEE Control Systems Magazine, 2009, 29(5), 22-30.
The original publication is available at http://ieeexplore.ieee.org/
doi : 10.1109/MCS.2009.933524

(a)

(b)

(c)

Figure 7: Gignac canal. The main canal is 50 km long, with a feeder canal of 8 km, and two branches on both the left and right banks of Hérault river. The left branch, which is 27 km long, and the right branch, which is 15 km long, originate at the Partiteur station. (a) shows the left and right branches of Partiteur station. (b) shows an automatic regulation gate at the right branch used to control the water discharge. (c) shows the ultrasonic velocity sensor that measures the average water velocity. (Photo courtesy of David Dorchies.)

Author-produced version of the article published in IEEE Control Systems Magazine, 2009, 29(5), 22-30.
The original publication is available at http://ieeexplore.ieee.org/
doi : 10.1109/MCS.2009.933524

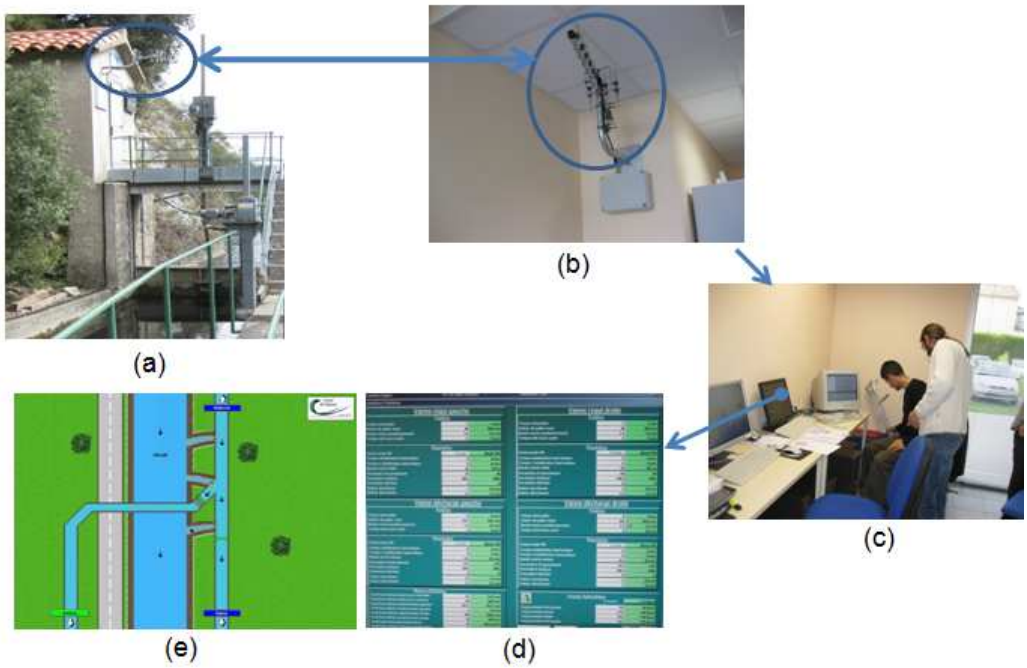

Figure 8: SCADA (supervision, control, and data acquisition) system. The SCADA system manages the canal by enabling the monitoring of the water discharge and by controlling the actuators at the gates. Data from sensors and actuators on the four gates at Partiteur are collected by a control station equipped with an antenna (a). The information is communicated by radio frequency signals every five minutes to a receiving antenna (b), located in the main control center, a few kilometers away (c). The data are displayed and saved in a database, while commands to the actuators are sent back to the local controllers at the gates (d)-(e). The SCADA performs open-loop control in real time. (Photo courtesy of Tarek Rabbani.)

Author-produced version of the article published in IEEE Control Systems Magazine, 2009, 29(5), 22-30.
The original publication is available at http://ieeexplore.ieee.org/
doi : 10.1109/MCS.2009.933524

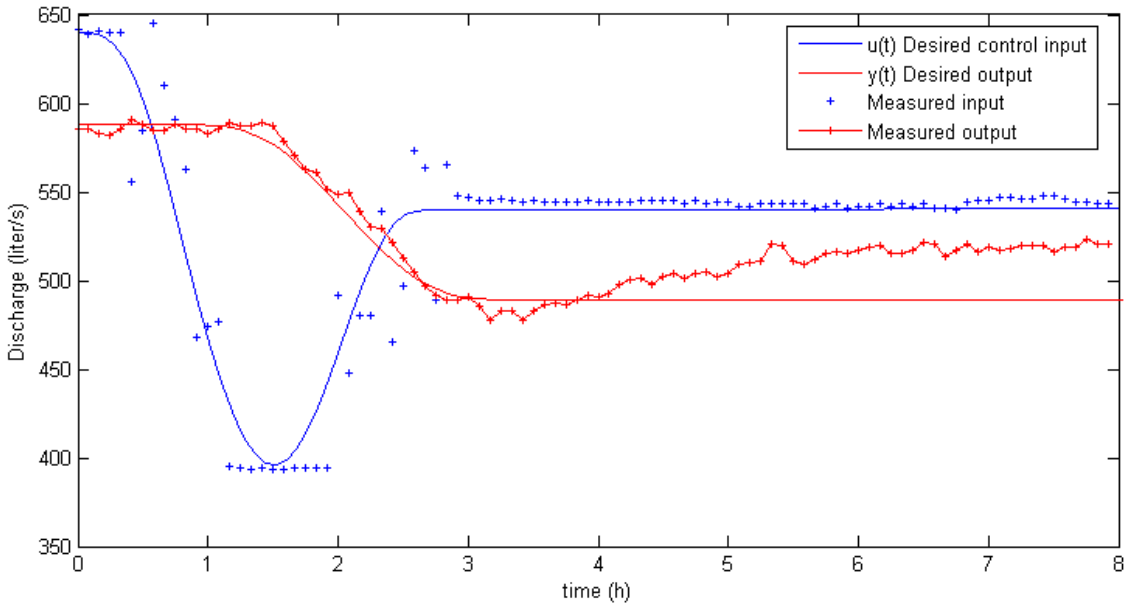

Figure 9: Implementation results of the Hayami controller on the Gignac canal. The Hayami open-loop control $u(t)$ is applied to the right branch of Partiteur using the SCADA system. The measured output (downstream water discharge) follows the desired curve, except at the end of the experiment. This discrepancy cannot be explained solely by the actuator limitations, but rather is due to simplifications in the model assumptions.

Author-produced version of the article published in IEEE Control Systems Magazine, 2009, 29(5), 22-30.
The original publication is available at http://ieeexplore.ieee.org/
doi : 10.1109/MCS.2009.933524

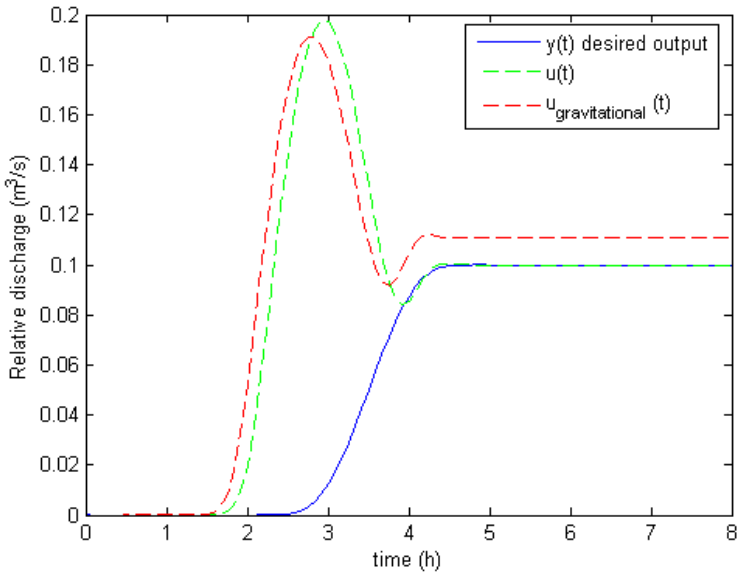

Figure 10: Hayami control taking into account the effect of gravitational lateral withdrawals. The control input is computed with the Hayami model (with constant and gravitational lateral withdrawals). As expected, to account for gravitational lateral withdrawals, the open-loop control $u_{\text{gravitational}}(t)$ needs to release more water than is required at the downstream end.

Author-produced version of the article published in IEEE Control Systems Magazine, 2009, 29(5), 22-30.
The original publication is available at http://ieeexplore.ieee.org/
doi : 10.1109/MCS.2009.933524

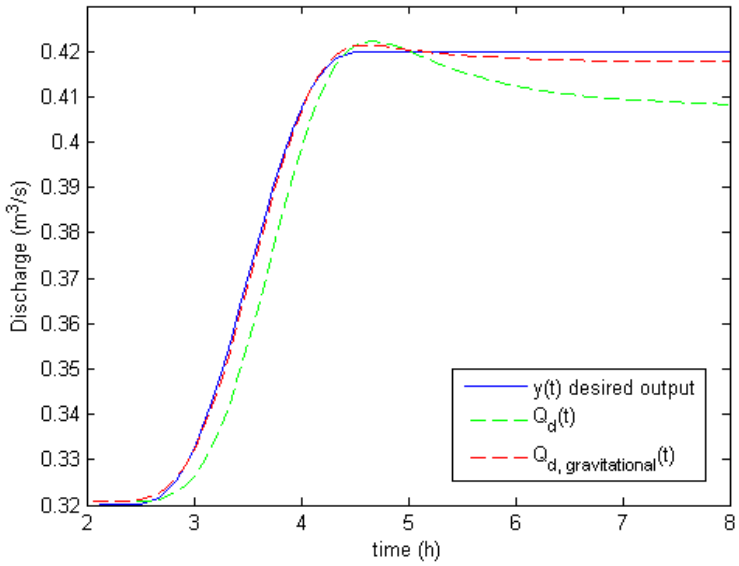

Figure 11: Comparison of the desired and simulated downstream water discharges. The downstream water discharge, $Q_d(t)$ and $Q_{d,\text{gravitational}}(t)$, is computed by solving the Saint-Venant equations with upstream water discharges $u(t)$ and $u_{\text{gravitational}}(t)$, respectively. Accounting for gravitational lateral withdrawals enables the controller to follow the desired output. This result is obtained on a realistic model of SIC, which is different from the simplified Hayami model used for control design.

Author-produced version of the article published in IEEE Control Systems Magazine, 2009, 29(5), 22-30.
The original publication is available at http://ieeexplore.ieee.org/
doi : 10.1109/MCS.2009.933524

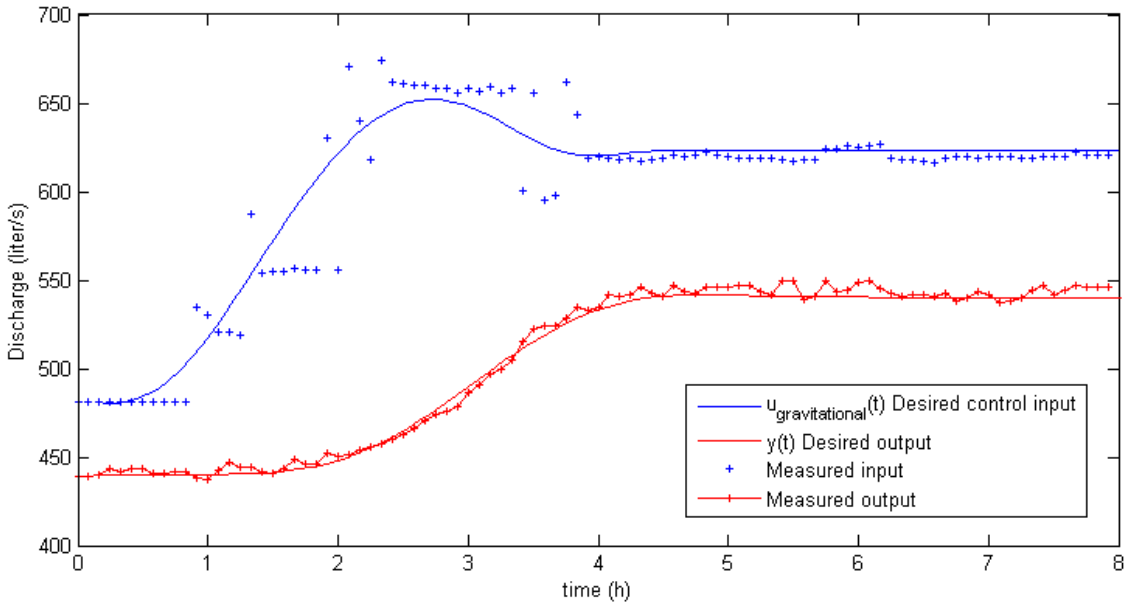

Figure 12: Implementation results of the Hayami controller on the Gignac canal. The Hayami controller assumes gravitational lateral withdrawals. The relative error between the measured downstream water discharge and the desired downstream water discharge is less than 9%, despite the fact that the delivered upstream water discharge is perturbed due to actuator limitations.

Author-produced version of the article published in IEEE Control Systems Magazine, 2009, 29(5), 22-30.
The original publication is available at http://ieeexplore.ieee.org/
doi : 10.1109/MCS.2009.933524

Sidebar 1: What is Differential Flatness?

The theory of differential flatness consists of a parameterization of the trajectories of a system by one of its outputs, called the *flat output* and its derivatives [S1]. Let us consider a system $\dot{x} = f(x, u)$, where the state x is in $\mathbb{R}^n$, and the control input u is in $\mathbb{R}^m$. The system is said to be *flat*, and admits the flat output z, where $\dim(z) = \dim(u)$ and the state x can be parameterized by z and its derivatives. More specifically, the state x can be written as $x = h(z, \dot{z}, ..., z^{(n)})$, and the equivalent dynamics can be written as $u = g(z, \dot{z}, ..., z^{(n+1)})$.

In the context of partial differential equations, the vector x can be thought of as infinite dimensional. The notion of differential flatness extends to this case, and, for a differentially flat system of this type, the evolution of x can be parameterized using an input u, which often is the value of x at a given point. A system with a flat output can then be parameterized as a function of this output. This parameterization enables the solution of open-loop control problems, if this flat output is the one that needs to be controlled. The open-loop control input can then directly be expressed as a function of the flat output. This parameterization also enables the solution of motion planning problems, where a system is steered from one state to another. Differential flatness is used to investigate the related problem of motion planning for heavy chain systems [S2], as well as the Burgers equation [S3], the telegraph equation [S4], the Stefan equation [S5], and the heat equation [S6].

Parameterization can be achieved in various ways depending on the type of the problem. Laplace transform is widely used [S2], [S3], [S4] to invert the system. The equations can be transformed back from the Laplace domain to the time domain, thus resulting in the flatness

Author-produced version of the article published in IEEE Control Systems Magazine, 2009, 29(5), 22-30.
The original publication is available at http://ieeexplore.ieee.org/
doi : 10.1109/MCS.2009.933524

parameterization. Alternative methods can be used to compute the parameterization in the time domain directly. For example, the Cauchy-Kovalevskaya form [S6], [S7] parameterizes the solution of a partial differential equation in $X(\zeta, t)$, where $\zeta \in [0, 1]$ and $t \in [0, \infty)$, as a power series in space multiplied by time-varying coefficients, that is, $X(\zeta, t) = \sum_{i=0}^{\infty} a_i(t) \frac{\zeta^i}{i!}$. Here, $X(\zeta, t)$ is the state of the system and $a_i(t)$ is a time function. The usual approach is to substitute the Cauchy-Kovalevskaya form in the governing partial differential equation and boundary conditions to obtain a relation between $a_i(t)$ and the flat output $y(t)$ or its derivatives, for example, $a_i(t) = y^{(i)}(t)$, where $y^{(i)}(t)$ is the i^{th} derivative of $y(t)$, which leads to the final parameterization, in which $a_i(t)$ is written in terms of the desired output $y(t)$.

References

[S1] M. Fliess, J.L. Lévine, P. Martin, and P. Rouchon. Flatness and defect of non-linear systems: introductory theory and examples. *International Journal of Control,* 61(6):1327–1361, 1995.

[S2] N. Petit and P. Rouchon. Flatness of heavy chain systems. *SIAM Journal on Control and Optimization,* 40 (2):475–495, 2001.

[S3] N. Petit, Y. Creff, P. Rouchon, and P. CAS-ENSMP. Motion planning for two classes of nonlinear systems with delays depending on the control. *Proceedings of the 37th IEEE Conference on Decision and Control, Tampa, FL,* 1:1007–1011, December 1998.

[S4] M. Fliess, P. Martin, N. Petit, and P. Rouchon. Active signal restoration for the telegraph equation. *Proceedings of the 38th IEEE Conference on Decision and Control, Phoenix,* 2:1107–1111, 1999.

Author-produced version of the article published in IEEE Control Systems Magazine, 2009, 29(5), 22-30.
The original publication is available at http://ieeexplore.ieee.org/
doi : 10.1109/MCS.2009.933524

[S5] W. Dunbar, N. Petit, P. Rouchon, and P. Martin. Motion planning for a nonlinear Stefan problem. *ESAIM: Control, Optimisation and Calculus of Variations,* 9:275–296, 2003.

[S6] B. Laroche, P. Martin, and P. Rouchon. Motion planning for the heat equation. *International Journal of Robust and Nonlinear Control,* 10(8):629–643, 2000.

[S7] B. Laroche, P. Martin, and P. Rouchon. Motion planning for a class of partial differential equations with boundary control. *Proceedings of the 37th IEEE Conference on Decision and Control, Tampa, FL,* 3:3494–3497, 1998.

Author-produced version of the article published in IEEE Control Systems Magazine, 2009, 29(5), 22-30.
The original publication is available at http://ieeexplore.ieee.org/
doi : 10.1109/MCS.2009.933524

Sidebar 2: How to Impose a Discharge at a Gate?

Once a desired open-loop water discharge rate is computed, it needs to be imposed at the upstream end of the canal. In open-channel flow, it is not easy to impose a water discharge rate at a gate. Indeed, once a gate is opened or closed, the upstream and downstream water levels at the gate change quickly and modify the water discharge rate, which is a function of the water levels on both sides of the gate. One possibility would be to use a local slave controller that operates the gate in order to deliver a given water discharge rate. But due to operational constraints, it is usually not possible to operate the gate at a high sampling rate. As an example, some large gates cannot be operated more than few times an hour because of motor constraints, which directly limits the operation of the local controller.

Several methods have been developed by hydraulic engineers to perform this control input based on the gate equation (S1), which provides a good model for the flow through the gate [S8]. The problem can be described as depicted in Figure S1. Two pools are interconnected with a hydraulic structure, a submerged orifice (also applicable for more complex structures). The gate opening is to be controlled to deliver a required flow from pool 1 to pool 2.

The hydraulic cross structure is modeled by a static relation between the water discharge through the gate Q, the water levels upstream and downstream of the gate Y_1 and Y_2, respectively, and the gate opening W given by

$$Q = C_d \sqrt{2g} L_g W \sqrt{Y_1 - Y_2}, \tag{S1}$$

where C_d is a discharge coefficient, L_g is the gate width, and g is the gravitational acceleration. This nonlinear model can be linearized for small deviations q, y_1, y_2, w from the reference water

Author-produced version of the article published in IEEE Control Systems Magazine, 2009, 29(5), 22-30.
The original publication is available at http://ieeexplore.ieee.org/
doi : 10.1109/MCS.2009.933524

discharge value Q, water levels Y_1, Y_2, and gate opening W, respectively. This linearization leads to the equation

$$q = k_u (y_1 - y_2) + k_w w,$$

where the coefficients k_u and k_w are obtained by differentiating (S1) with respect to Y_1, Y_2, and W, respectively.

Various inversion methods can be applied either to the nonlinear or to the linear model to obtain a gate opening W necessary to deliver a desired water discharge through the gate, usually during a sampling period T_s. The static approximation method assumes constant water levels Y_1 and Y_2 during the gate operation period T_s. This approximation leads to an explicit solution of the gate opening W in the linear model assumption. The characteristic approximation method uses the properties for zero-slope rectangular frictionless channel to approximate the water levels. The linear version of the model also leads to an explicit expression for the gate opening. The dynamic approximation method uses the linearized Saint-Venant equations to predict the water levels. This method can be thought of as a global method because it considers the global dynamics of the canal to predict the gate opening necessary to deliver the desired flow. In [S8], the three methods are compared by simulation and tested by experimentation on the Gignac canal. The dynamic approximation method has been shown to better predict the gate opening necessary to obtain the desired average water discharge [S8].

References

[S8] X. Litrico, P.-O. Malaterre, J.-P. Baume, and J. Ribot-Bruno. Conversion from discharge to gate opening for the control of irrigation canals. *Journal of Irrigation and Drainage*

Engineering, 134(3):305–314, 2008.

Author-produced version of the article published in IEEE Control Systems Magazine, 2009, 29(5), 22-30.
The original publication is available at http://ieeexplore.ieee.org/
doi : 10.1109/MCS.2009.933524

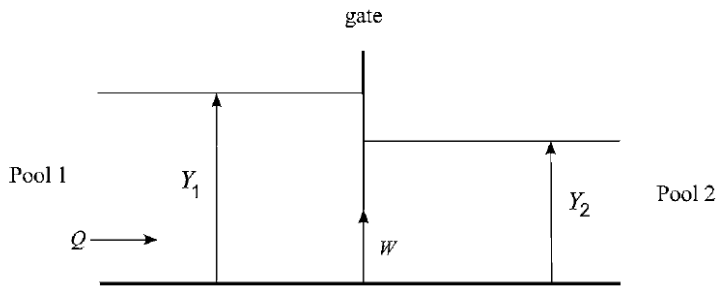

Figure S1: Gate separating two pools. The gate opening W controls the water flow from Pool 1 to Pool 2. The water discharge can be computed from the water levels Y_1, Y_2, and the gate opening W [S8].

Author-produced version of the article published in IEEE Control Systems Magazine, 2009, 29(5), 22-30.
The original publication is available at http://ieeexplore.ieee.org/
doi : 10.1109/MCS.2009.933524

Author Information

Tarek Rabbani (trabbani@berkeley.edu) completed the Engineering Degree in mechanical engineering from American University of Beirut, Lebanon and the M.S. degree in mechanical engineering from the University of California, Berkeley. He is a Ph.D. student in mechanical engineering at the University of California at Berkeley. He held a visiting researcher position at NASA Ames Research Center in the summer of 2008. His research focuses on control of irrigation canals and air traffic management.

Simon Munier completed the Engineering Degree in hydraulics and fluid mechanics from the ENSEEIHT (Ecole Nationale Supérieure d'Electronique, d'Electrotechnique, d'Informatique, d'Hydraulique et de Telecommunication) in France. He is currently finishing the Ph.D. at Cemagref on integrated modeling methods for the control of watershed systems.

David Dorchies completed the Engineering Degree from the National School for Water and Environmental Engineering of Strasbourg in 2005. Between September 2005 and September 2008, he worked in the construction and rehabilitation of waste-water networks and waste water treatment plant at Poitiers for the Ministry of Agriculture. Since September 2008, he worked in the TRANSCAN Research Group, which deals with Rivers and Irrigation Canals Modeling and Control.

Pierre-Olivier Malaterre completed the Engineering Degree in mathematics, physics and computer science from the Ecole Polytechnique in France from 1984 to 1987. He then joined the GREF public body with specialization in water management. He completed the masters degree in hydrology in 1989 at Engref and University of Jussieu in Paris. His masters was a collaboration

Author-produced version of the article published in IEEE Control Systems Magazine, 2009, 29(5), 22-30.
The original publication is available at http://ieeexplore.ieee.org/
doi : 10.1109/MCS.2009.933524

with Cemagref in Montpellier and the International Water Management Institute in Sri Lanka. He joined Cemagref in 1989, where he contributed to the development of the SIC software and completed, in parallel, the Ph.D. with the LAAS (Laboratoire d'Automatique et d'Analyse des Systèmes) in Toulouse and the Engref Engineering School in 1994. He held a visiting researcher position in the control group of the Iowa State University in 1999-2000. He is the Transcan Research Group leader at Cemagref Montpellier from 1995, where his research focuses on modeling and control of open-channel hydraulic systems such as rivers and irrigation canals.

Alexandre Bayen received the Engineering Degree in applied mathematics from the Ecole Polytechnique, France, in July 1998, the M.S.and Ph.D. degrees in aeronautics and astronautics from Stanford University in June 1999, and December 2003. He was a visiting researcher at NASA Ames Research Center from 2000 to 2003. Between January 2004 and December 2004, he worked as the Research Director of the Autonomous Navigation Laboratory at the Laboratoire de Recherches Balistiques et Aerodynamiques, (Ministere de la Defense, Vernon, France), where he holds the rank of Major. He has been an assistant professor in the Department of Civil and Environmental Engineering at UC Berkeley since January 2005. He is the recipient of the Ballhaus Award from Stanford University, 2004. His project Mobile Century received the 2008 Best of ITS Award for 'Best Innovative Practice', at the Intelligent Transportation Systems (ITS) World Congress in New Work. He is a recipient of a CAREER award from the National Science Foundation, 2009.

Xavier Litrico received the Engineering Degree in applied mathematics from the Ecole Polytechnique, France, in July 1993, the M.S. and Ph.D. degree in water sciences from the Ecole Nationale du Génie Rural, des Eaux et des Forêts in 1995 and 1999, and the "Habilitation à Diriger des

Author-produced version of the article published in IEEE Control Systems Magazine, 2009, 29(5), 22-30.
The original publication is available at http://ieeexplore.ieee.org/
doi : 10.1109/MCS.2009.933524

Recherches" in control engineering from the Institut National Polytechnique de Grenoble in 2007. He has been with Cemagref (French Public Research Institute on Environmental Engineering) since 2000. He was a visiting scholar at the University of California at Berkeley in 2007-2008. His main research interests are modeling, identification, and control of hydrosystems such as irrigation canals or regulated rivers. He can be contacted at UMR G-EAU, Cemagref, 361 rue JF Breton, BP 5096, F-34196 Montpellier Cedex 5, France.